Polymer Chemistry

Accepted Manuscript

ROYAL SOCIETY OF CHEMISTRY

www.rsc.org/polymers

Cite this: DOI: 10.1039/c0xx00000x

www.rsc.org/xxxxxx

ARTICLE TYPE

"Clickable" Thiol-Functionalized Nanoporous Polymers: From their Synthesis to Further Adsorption of Gold Nanoparticles and Subsequent Use as Efficient Catalytic Supports

Benjamin Le Droumaguet,* Romain Poupart & Daniel Grande

Received (in XXX, XXX) Xth XXXXXXXXX 20XX, Accepted Xth XXXXXXXXX 20XX
DOI: 10.1039/b000000x

A straightforward and versatile approach towards thiol-functionalized nanoporous polystyrene frameworks is reported through the selective cleavage of a disulfide bridge at the junction between both blocks of newly synthesized polystyrene-*block*-poly(D,L-lactide) (PS-*b*-PLA) diblock copolymer precursors. This methodology requires the synthesis of a disulfide-bearing heterodifunctional initiator that allows for the production of well-defined diblock copolymers by combining atom transfer radical polymerization (ATRP) of styrene and ring-opening polymerization (ROP) of D,L-lactide. After macroscopic orientation of the copolymer precursors through channel die processing and subsequent quantitative degradation of the disulfide bridge *via* triphenylphosphine-mediated reduction, thiol-functionalized porous polymers are obtained. Further, "click" thiol-ene-mediated functionalization of thiol-coated pore walls within nanoporous frameworks is implemented. More interestingly, adsorption of *in-situ* generated gold nanoparticles and subsequent and unprecedented supported catalytic reduction of a model nitroaromatic compound, *i.e. para*-nitrophenol, are successfully achieved. Reusability of the hybrid catalyst is also proved over a 5 run-cycle with conversion of nearly 70% within only two hours.

Introduction

Due to the large variety of properties and applications of organic porous materials,[1] nanoporous polymer-based systems have attracted significant attention within the research community. The applications for these materials are diverse, *i.e.* filtration and separation techniques, heterogeneous supported catalysis, as well as diagnosis or drug delivery.[2, 3] Organic porous materials present unique properties compared to their inorganic nanostructured analogues,[4] such as simplicity of functionalization, tunable mechanical properties, and above all low-cost production. The preparation of porous polymeric materials has been reported with pore sizes ranging from some nanometers to some micrometers. More interestingly, block copolymers (BCPs) develop well-defined equilibrium domain morphologies (*i.e.*, for linear diblock copolymers, alternating lamellae, hexagonally close-packed cylinders, bicontinuous gyroids, and body-centered cubic spheres), and thus constitute arguably ideal nanostructured precursors for the formation of ordered mesoporous polymers.[5-7] In this particular case, the copolymer is composed of at least one sacrificial block that should allow for well-defined porosity after a selective etching process. The removal of the sacrificial block can be achieved using two main strategies. The first one relies on the degradation of the expendable segment itself. In this case, etching conditions are clearly dictated by the nature of the concerned block. The sacrificial components used to generate nanopores in BCP precursors are diversified and include poly(dimethylsiloxane) (PDMS),[8-10] poly(propylene glycol) (PPG),[11] polyisoprene (PI)[12] or poly(methyl methacrylate) (PMMA)[13, 14] that can be degraded by reaction with HF or tetrabutyl ammonium fluoride, oxygen plasma treatment (or degradation in presence of fuming nitric acid), ozonolysis or UV irradiation followed by acetic acid extraction, respectively. In addition, the selective hydrolysis of the polyester block associated with polystyrene-*block*-poly(D,L-lactide) (PS-*b*-PLA) diblock copolymers has allowed for controlling the porosity and the functionality of resulting nanoporous polymers, in previous contributions.[15-18] Alternatively, ongoing research concerns the development of more efficient and environmentally benign etching strategies. In this context, the insertion of an easily cleavable linker group at the junction between the microphase-separated blocks of BCPs seems to be a promising route, since it allows for site-specific scission between both blocks. This elegant strategy does not require degradation of the entire backbone of the polymer segment in the sacrificial minor phase. The chemical nature of the linker should thus be suitably chosen so as to allow for its subsequent cleavage under experimental conditions that do not alter/destroy the morphology of BCPs obtained during the self-organization process. "Smart" methodologies involving the cleavage of the chemical junction between incompatible blocks have been successfully put forward in the literature for the generation of nanoporous polymeric frameworks. For instance, a hetero-Diels-Alder adduct,[19] orthonitrobenzyl,[20, 21] or trityl ether[22] functional groups can be inserted at the junction between both blocks of diblock copolymers, and such groups can be specifically cleaved under rather mild conditions. A ruthenium (II)-terpyridine bis-complex[23] or a $-SO_3^-@-NH_3^+$ ionic pair[24] have also been introduced into "pseudo" BCPs, allowing for further facile degradation of the interfacial junction moiety. Such design strategies for the incorporation of a functional junction essentially do not alter the self-organization behaviour of the BCPs because of the negligible volume fraction of the linking entities. Moreover, they pave the way for decoration of pore walls with reactive functional groups and expand the choice of components for the BCP precursors. Especially, the chemical reduction of a disulfide bridge at the junction between incompatible polystyrene (PS) and poly(ethylene oxide) (PEO) segments in PS-*b*-PEO copolymers has afforded well-defined nanoporous polystyrene frameworks.[25] Nevertheless, the preparation of such advanced materials requires many synthetic steps so as to introduce the disulfide bridge within the diblock copolymer precursors.

In this context, we describe the synthesis of PS-*b*-PLA diblock copolymers possessing a disulfide group at the junction point between both blocks *via* a novel and straightforward methodology from a purposely designed disulfide-bearing dual initiator. Their macroscopic orientation, followed by the reduction of the disulfide bridge joining both blocks leads to the formation of nanoporous polymeric materials with thiol-coated pore walls. The subsequent "click" thiol-ene coupling with a model allyl-functionalized PEG evidences the presence of chemically accessible and modifiable thiol functions on the pore surface. Furthermore, *in-situ* generated gold nanoparticles (GNPs) are immobilized at the surface of nanochannels, and these innovative hybrid systems can efficiently be used as supported catalysts. To the best of our knowledge, such GNP@nanoporous polymer hybrid materials have not found any application as nanoreactors in heterogeneous catalysis so far.

Experimental

Materials

All polymerizations were carried out using standards Schlenk techniques under nitrogen atmosphere. THF (99.9%, SDS) and anisole (99%, SDS) were stored upon 4 Å molecular sieves, and used without any further purification. Prior to use, Cu(I)Br (99%, Aldrich) was purified as reported by Keller and Wycoff.[26] Styrene (Aldrich) was passed through a column filled with basic alumina in order to remove any polymerization inhibitor. Pentamethyldiethylenetriamine (PMDETA, 99%, Aldrich), 3,6-dimethyl-1,4-dioxane-2,5-dione (D,L-lactide, LA), bis(2-hydroxyethyl) disulfide (technical grade, 90%), α-bromoisobutyryl bromide (98%), tin(II) 2-ethylhexanoate ($Sn(Oct)_2$, 95%), triethylamine (99%), gold(III) chloride hydrate ($AuCl_3 \bullet xH_2O$, 99.999%), $NaBH_4$ and allyl bromide (ReagentPlus®, 99%) were purchased from Aldrich and used as received. 4-nitrophenol was supplied by Alfa Aesar. Triphenylphosphine (99%, Acros), dichloromethane (99.9%, Carlo Erba), anhydrous toluene (99.8%, Aldrich), and methanol (MeOH, 99%, SDS) were used without any further purification. α-methoxy poly(ethylene glycol) ($M_{n\ NMR}$ = 590 $g.mol^{-1}$) was obtained from Aldrich and used as received.

18.2 MΩ deionized water was filtered through a Milli-Q Plus purification pack.

Synthesis of 2-[(2-hydroxyethyl)dithio]ethyl 2-bromoisobutyrate

2-[(2-hydroxyethyl)dithio]ethyl 2-bromoisobutyrate was synthesized according to a modified literature procedure.[12] 15.39 g (0.099 mol) of bis(2-hydroxyethyl) disulfide, 100 mL of THF, and 12.54 mL (0.090 mol) of triethylamine were introduced into a three-neck round bottom flask kept under nitrogen atmosphere. The reaction mixture was cooled to 0 °C. 11 mL (0.089 mol) of α-bromoisobutyryl bromide were added dropwise overnight. The reaction mixture was finally stirred at 50 °C for 5 h. After removal of the solvent, the crude product was purified by silica gel column chromatography with an eluent mixture, *i.e.* dichloromethane / cyclohexane (1/3 to 1/1 v/v). The pure product was obtained as a viscous yellowish oil. Yield: 58%. ^1H NMR ($CDCl_3$, 400 MHz, 298 K): δ (ppm): 1.92 (s, 6H, $-C(CH_3)_2-Br$), 2.88 (t, 2H, $HO-CH_2-CH_2-S-$, ^3J = 5.8 Hz), 2.96 (t, 2H, $-CO-O-CH_2-CH_2-S-$, ^3J = 6.7 Hz), 3.88 (t, 2H, $HO-CH_2-$, ^3J = 5.8 Hz), 4.39(t, 2H, $-C{=}O-O-CH_2-$, ^3J = 6.7 Hz) ; ^{13}C NMR ($CDCl_3$, 100 MHz, 298 K) : δ (ppm) : 31.07 (2C, $C-(CH_3)_2$), 36.87 (1C, $HO-CH_2-CH_2-$) , 41.80 (1C, $-S-CH_2-CH_2-O-CO-$), 55.95 (1C, $HO-CH_2-$), 68.73 (1C, $-CH_2-O-CO-$), 171.97 (1C, $-CO_2-$) . Elemental analysis calculated for $C_8H_{15}BrO_3S_2$: C 31.69%, H 4.99%, Br 26.35%, O 15.83%, S 21.15%; found C 31.41%, H 4.68%, Br 25.60%, O 19.51%, S 18.80%.

Preparation of polystyrene macroinitiator (PS_{104}-OH)

Styrene (11 g, 0.105 mol), 2-[(2-hydroxyethyl)dithio]ethyl 2-bromoisobutyrate (0.304 g, 1 mmol), anisole (4 mL), CuBr (145 mg, 1 mmol) and DMSO (2 mL) were added in a dry Schlenk flask carefully purged with nitrogen. The reaction mixture was degassed by three freeze-pump-thaw cycles before adding PMDETA (120 µL, 1 mmol) under N_2 atmosphere. The initial ratio [monomer]:[initiator]:[ligand]:[catalyst] of the atom transfer radical polymerization (ATRP) feed was fixed at 100:1:1:1 so as to obtain a PS_{104}-OH macroinitiator with a theoretical $M_n \sim 10$ $kg.mol^{-1}$ after virtually total conversion of the monomer. The flask was immersed in an oil bath at 110 °C. After 36 h, the reaction medium was diluted with CH_2Cl_2, passed through a small pad of neutral alumina and precipitated at least twice into a large volume of cold methanol. The as-obtained PS-OH macroinitiator was dried under vacuum to afford a fine white off powder that was further characterized by ^1H NMR and SEC analyses.

Microwave-assisted synthesis of PS-*b*-PLA diblock copolymers

The microwave-assisted ring-opening polymerization (ROP) of LA was carried out using an Anton-Paar monomode 300 microwave reactor. The microwave source was a magnetron with a 2.45 GHz frequency powered by a 900 W power generator, which

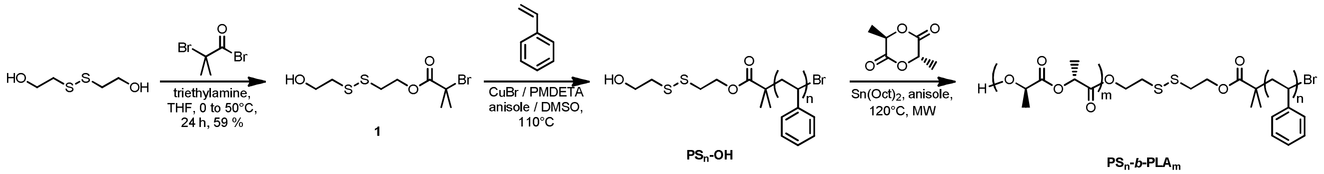

Figure 1. Synthetic pathway towards PS-*b*-PLA diblock copolymer precursors by a tandem approach combining ATRP of styrene and MW-assisted ROP of D,L-lactide initiated by 2-[(2-hydroxyethyl)dithio]ethyl 2-bromoisobutyrate.

could be operated at different power levels. Typically, 500 mg (4.8 mmol) of PS$_{104}$-OH and 660 mg (4.6 mmol) of LA were dissolved in 1 mL of anhydrous toluene in a 10 mL microwave-transparent quartz vial, and the mixture was freeze-dried overnight.[27, 28] After freeze-drying, 1 mL of anisole and 50 µL of Sn(Oct)$_2$ (4.8 mmol) were added under a dried nitrogen flow, and the vial was closed with a silicon cap. The internal reaction temperature (120 °C) was monitored and controlled with a fiber-optic sensor (Ruby thermometer) immersed in the reaction solution under vigorous stirring. The polymerization was terminated by cooling the vial with compressed air. The product was diluted with CH$_2$Cl$_2$, and precipitated at least twice into a large volume of methanol. The as-obtained PS-*b*-PLA copolymer was dried under vacuum. It was further analyzed by SEC and ^{1}H NMR analyses.

Orientation of PS-*b*-PLA diblock copolymers

A home-made channel die (3 mm wide and 60 mm long) was used to align the nanodomains in the block copolymers. Previously pressed pieces of PS-*b*-PLA were placed in the center of the channel die which was then heated to 140 °C in a laboratory press. The samples were subjected to compression upon constant load (compression ratio of ~ 10) and quenched under load to room temperature over a period of 1 h. The samples were post-annealed overnight at 160 °C to reach thermodynamic equilibrium, before removing them from the channel die with a sample thickness between 0.5 and 1.0 mm.

Removal of PLA segment in diblock copolymers by reduction of disulfide bond

In order to selectively get rid of the PLA block, PS-*b*-PLA pieces (200 mg) were immersed in a mixture containing 6 mL of ethanol and 600 mg of triphenylphosphine at 65 °C for 5 days. The as-obtained porous samples were washed abundantly with ethanol. After dissolution of the sample in CDCl$_3$, the selective removal of the PLA block by reduction of the disulfide bridge was confirmed by ^{1}H NMR.

Synthesis of allyl-terminated poly(ethylene glycol)

An allyl-functionalized poly(ethylene glycol) (PEG) sample was prepared following a previously reported experimental procedure: It was synthesized by reacting a 590 g.mol^{-1} PEG oligomer (1 g, 1.82 mmol) with an excess of allyl bromide (440 mg, 3.64 mmol) over 145 mg of NaOH powder in 5 mL toluene for 12 h at 45 °C.[29] At the end of the reaction, toluene was removed under reduced pressure. The residue was dissolved with 10 mL of deionized water. The aqueous phase was extracted with 4 × 20 mL water. Pooled organic fractions were dried over MgSO$_4$, and CH$_2$Cl$_2$ was finally removed under reduced pressure. The pure product was obtained as a pale yellow oil (yield ~ 100%). ^{1}H NMR (CDCl$_3$, 400 MHz, 298 K) δ (ppm): 5.96–5.82 (m, 1H, CH$_2$=C*H*–CH$_2$–), 5.20 (dd, 2H, C*H$_2$*=CH–CH$_2$–, J = 16 & 40 Hz), 3.99 (d, 2H, CH$_2$=CH–C*H$_2$*–), 3.48–3.75 (m, 52 H, –O–C*H$_2$*–C*H$_2$*–O–), 3.35 (s, 3H, –O–C*H$_3$*).

End-group functionalization by thiol-ene "click" chemistry

In a 10 mL round-bottom flask, 20 mg of PS$_{104}$-SH (1.45.10^{-4} mol, 1 equiv.) was suspended in a 1 mol % AIBN solution in ethanol (3 mL). 6 mg of allyl-terminated PEG (5.8. 10^{-4} mol, 5 equiv.) was added to the suspension. The reaction mixture was stirred for 24 h at 90 °C. The product was recovered by filtration after abundant washing with ethanol and analyzed by ^{1}H NMR.

In-situ generation of gold nanoparticles by reducing HAuCl$_4$

21.7 mg of nanoporous polystyrene were put into 1 mL of a 0.1 wt% HAuCl$_4$ solution over 3 days. 5 mg of NaBH$_4$ in 10 mL of water was added dropwise and permitted to react for 2 h. The sample was vigorously washed with water to remove unadsorbed gold nanoparticles (GNPs). SEM pictures of the samples were recorded to check the nanoparticle immobilization.

Reduction of 4-nitrophenol by supported heterogeneous catalysis

A freshly prepared solution containing 200 µL of 4-nitrophenol (5 mg in 10 mL of deionized water), 200 µL of NaBH$_4$ (114 mg in 10 mL of water) in 4 mL of water was mixed with 10 mg of the as-obtained supported GNP-based catalyst for 2 h at room temperature in dark conditions. UV-Vis spectra were recorded before the catalyst addition and 2 h after addition in order to determine the reaction yield. For the sake of comparison, a 4 mL solution containing 200 µL of NaBH$_4$ (114 mg in 10 mL of water) and 200 µL of a 4-nitrophenol solution (5 mg in 10 mL of water) was left for 2 h in the presence of thiol-functionalized nanoporous frameworks as a blank experiment. An iteration of 5 successive cycles was achieved through the same process, again in dark conditions. UV-Vis spectra were recorded in the same ways.

Instrumentation

Size Exclusion Chromatography (SEC) analyses were performed on a system equipped with a Spectra Physics P100 pump with two PL gel 5 µm mixed-C columns from Polymer Laboratories, and a Shodex RI 71 refractive index detector. The eluent was tetrahydrofuran at a flow rate of 1 mL.min^{-1}. The system was calibrated by using polystyrene standards from Polymer Source. ^{1}H and ^{13}C NMR spectra were recorded at room temperature on a Bruker Avance II spectrometer operating at a resonance frequency of 400 and 100 MHz, respectively. For ^{1}H NMR analysis, the sample concentration was ~10 mg. mL^{-1}, while it was ~ 30 mg.mL^{-1} for ^{13}C NMR experiments. $CDCl_3$ was used as solvent and internal standard (7.27 ppm in ^{1}H NMR; 77.2 ppm in ^{13}C NMR). Scanning Electron Microscopy (SEM) was performed on a LEO 1530 microscope equipped with InLens and Secondary Electron detectors using low accelerating voltage (3 kV). Prior to analyses, the samples were cryo-fractured and coated with a 3-nm layer of palladium/platinum alloy in a Cressington 208 HR sputter-coater. Energy-dispersive X-ray spectroscopy (EDX) was performed using an SSD X-Max detector of 50 mm^{2} from Oxford Instruments (127 eV for the Kα of Mn). Inductively coupled plasma optical emission spectrometry (ICP-OES) analysis was performed using a Varian Vista-PRO CCD Simultaneous spectrometer. UV-Vis spectra were recorded between 200 and 600 nm on a Cary 60 UV-Vis Spectrophotometer from Agilent Technologies.

Results and discussion

Synthesis of PS-*b*-PLA diblock copolymers

PS-*b*-PLA diblock copolymers with a disulfide bridge at the junction between both blocks were newly synthesized by an orthogonal tandem approach combining two distinct polymerization mechanisms, *i.e.* ATRP[30, 31] and ROP[32] (Figure 1).

Such a methodology required the employment of an asymmetric difunctional initiator for the generation of both blocks. For this purpose, we specifically prepared 2-[(2-hydroxyethyl)dithio]ethyl 2-bromoisobutyrate (HDBI **1**, Figure 1) because it contains *(i)* a disulfide bridge that can be easily cleaved *via* chemical reduction, *(ii)* a tertiary alkyl halide (C^{IV}–Br) that can initiate styrene ATRP, and *(iii)* a terminal primary hydroxyl group ($-CH_2OH$) that should ensure fast initiation for ROP of LA. This initiator (**1**) was prepared using an adapted literature procedure,[33, 34] and it was obtained in nearly 60% yield through a simple nucleophilic substitution by reaction of bis(2-hydroxyethyl) disulfide with 2-bromoisobutyryl bromide in the presence of triethylamine. ^{1}H and ^{13}C NMR analyses (Figure S1 ESI) along with elemental analysis of the pure compound confirmed the successful formation of the heterodifunctional initiator necessary to the synthesis of PS-*b*-PLA copolymer precursors. A polystyrene macroinitiator was obtained (PS_{104}-OH) from the initiator (**1**) and displayed an experimental M_n value close to the theoretical one along with a low molar mass dispersity $Đ$ (Table 1), thus confirming the controlled character of the ATRP of styrene. Further SEC (Figure S2) and ^{1}H NMR (Figure 2a) analyses corroborated the previous results. D,L-lactide was then polymerized from the as-obtained PS_{104}-OH macroinitiator (Table 1). The use of microwave-assisted ring-opening of D,L-lactide permitted to proceed with a fast polymerization kinetics (120 °C, 45 min),[27,28] while the polymerization lasted at least 5 days using a conventional heating process.[17] These PS-*b*-PLA copolymers where fully characterized by SEC (Figure S2) and ^{1}H NMR (Figure 2b); their main molecular characteristics are gathered in Table 1. It is noteworthy that these copolymer were synthesized with a PLA volume fraction (f_{PLA}) around 0.3–0.4 in order to develop a morphology of hexagonally close-packed PLA cylinders in a PS matrix, according to Hillmyer's previous investigations.[16] The ^{1}H NMR spectra displayed the typical chemical shifts of PS and PLA, the signals in the 6–7 ppm area being attributed to the aromatic protons of PS, and the resonance bands in the 5–5.5 ppm region arising from –CH– groups of PLA repeating units (Figure 2b)

Furthermore, Figure S2 (ESI) displays the typical SEC traces obtained for the PS macroinitiator and a PS-*b*-PLA copolymer. The SEC chromatogram of the copolymer exhibited a monomodal distribution and a peak shift toward a lower retention time, thus confirming the formation of a diblock copolymer, while the molar mass dispersity of the as-obtained PS-*b*-PLA copolymer remained rather narrow ($Đ < 1.3$).

Macroscopic orientation of diblock copolymers

The macroscopic orientation of PS-*b*-PLA copolymer nanodomains in bulk materials was realized using a channel die**.** processing technique, as reported elsewhere.[35] During this procedure, diblock copolymers were subjected to shear flow that induced a stress in the materials. This shear stress could then be relieved by a rearrangement of copolymers in such a way that the nanodomains might orientate along the shear direction.

Table 1. Molecular features of PS macroinitiator and PS-*b*-PLA precursors obtained using the asymmetric difunctional initiator HDBI (**1**).

PS_n[a] or PS_n-*b*-PLA_m[a]	Conversion[b] (%)	$M_{n\ theor}$[c] [kg/mol]	$M_{n\ NMR}$[d] [kg/mol]	$M_{n\ SEC}$[e] [kg/mol]	$Đ$[e]	Polymerization time [h]	f_{PLA}[f]
PS_{104-OH}	79	9.0	10.8	11.8	1.2	36	-
PS_{1O4}-*b*-PLA_{39}	35	15.9	16.5	23.6	1.3	0.75	0.29
PS_{1O4}-*b*-PLA_{47}	41	16.9	18.8	17.9	1.2	0.75	0.34
PS_{1O4}-*b*-PLA_{59}	54	18.8	20.0	20.8	1.2	0.75	0.38

[a] n, m : number-average polymerization degrees of PS or PLA blocks as determined by ^{1}H NMR

[b] Conversion as determined by gravimetry

[c] $M_{n\ theor}$ = conversion × DP_n × M_o(styrene) or $M_{n\ theor}$ = conversion × DP_n × M_o (LA) + $M_{n\ NMR}$ (PS-OH)

[d] $M_{n\ NMR}$: number-average molar mass evaluated by ^{1}H NMR

[e] SEC measurements with polystyrene standards

[f] Volume fraction of PLA as calculated by ^{1}H NMR, assuming that the densities of PS and PLA are 1.02 and 1.25, respectively

Cite this: DOI: 10.1039/c0xx00000x

www.rsc.org/xxxxxx

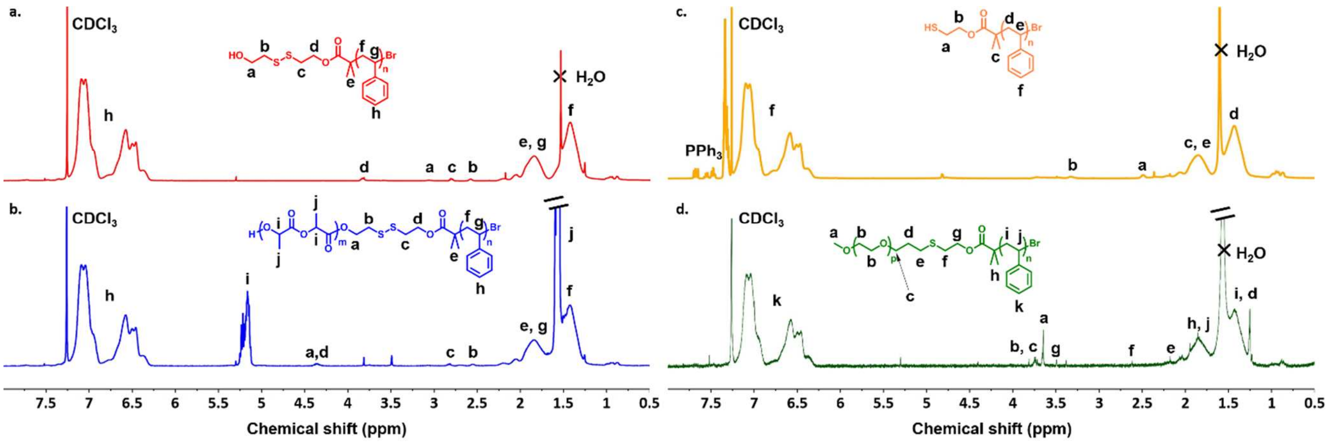

Figure 2. ^{1}H NMR spectra: (a) PS$_{104}$-OH macroinitiator prepared *via* ATRP, (b) PS$_{104}$-*b*-PLA$_{47}$ diblock copolymer prepared *via* the tandem ATRP-ROP approach, (c) PS$_{104}$-SH specimen after reductive degradation, (d) PS-SH coupled with PEG$_{14}$-allyl.
.

Generation of functionalized nanoporous polymeric materials

Phosphines, *e.g.* tributylphosphine, tris(2-carboxyethyl) phosphine and triphenylphosphine, are prone to efficiently reduce disulfide bridges, especially when inserted in the chemical structure of macromolecular architectures.[34,36-40] As a consequence, triphenylphosphine (PPh$_3$) was used to reduce the disulfide bridge at the junction between PS and PLA segments of the newly synthesized copolymers. This degradation was conducted in mild conditions, at 65 °C, namely an intermediate temperature between the T_g of PLA (around 50 °C) and that of PS (around 100 °C) in ethanol, *i.e.* a non-solvent for PS, and a solvent for PLA. The completion of this chemical cleavage was monitored by ^{1}H NMR after abundant washing of the resulting materials, drying, and subsequent solubilization in CDCl$_3$. Experimentally, within 5 days of reaction, the total disappearance of typical PLA bands (in particular the signal associated with –CH– protons of repeating units at 5.1–5.2 ppm), was observed as shown in Figure 2c, thus confirming the relatively fast completion of the chemical reduction. The experimental conditions selected afforded thiol-functionalized porous PS suitable for further coupling of model compounds *via* thiol-ene "click" chemistry.

Morphological and pore surface chemical characterization of nanoporous polymer frameworks

Upon disulfide reduction, the resulting materials obtained after removal of the PLA block displayed nanoporous frameworks as observed by SEM. The occurrence of well-defined nanoporosity (D_p = 10 nm) was confirmed by SEM with the observation of cylindrical nanopores (Figure 3), demonstrating the gain of the expected hexagonally close-packed cylindrical morphology. More importantly, an EDX analysis revealed the presence of sulfur atoms on the pore surface, as observed in Figure 4 with the presence of a weak signal for sulfur at 2.307 keV. Concomitantly, elemental analysis was conducted on the PS$_{104}$-OH macroinitiator, the PS$_{104}$-*b*-PLA$_{47}$ copolymer sample, and the corresponding PS material after reduction of disulfide bridge. The sulfur contents found by this technique were in good agreement with those theoretically calculated, *i.e.* 0.56, 0.32, and 0.28 wt.% for the experimental values found for the macroinitiator, the copolymer precursor, and the nanoporous polymer after reduction, and respectively 0.60, 0.34, and 0.30 wt.% for the expected values. These results thus corroborated the quantitative removal of PLA block during the disulfide bridge reduction step. In order to further demonstrate the availability of unmodified thiol groups on pore walls, a post-functionalization reaction was implemented.

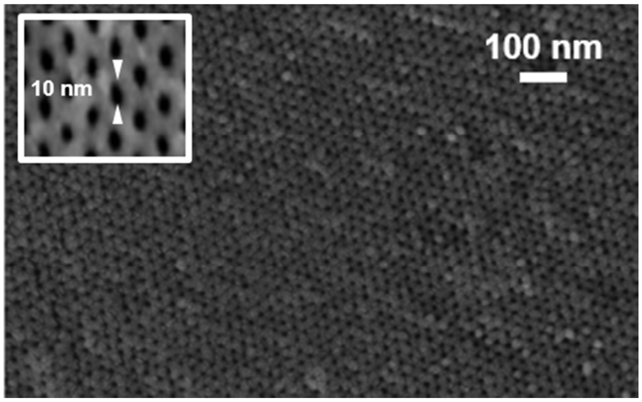

Figure 3. Cross-sectional SEM micrograph of the porous polymeric material obtained from PS$_{104}$-*b*-PLA$_{59}$ after channel die processing and removal of the PLA sacrificial block by selective PPh$_3$-mediated reduction of disulfide junction. Inset: zoom of the nanopore array (D_p = 10 nm).

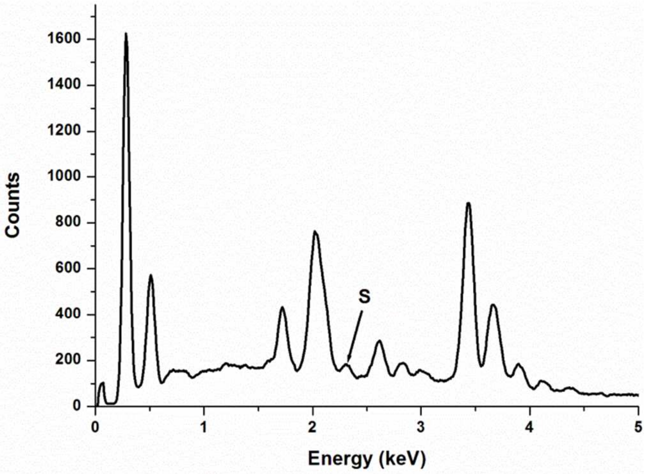

Figure 4. EDX spectrum of the pore surface of a thiol functionalized porous polystyrene obtained from a PS$_{104}$-*b*-PLA$_{47}$ diblock copolymer precursor.

Thiol-ene mediated functionalization of nanoporous PS frameworks

The presence of thiol functional groups as chain ends was confirmed through a post-modification "click" thiol-ene addition[41] in a heterogeneous medium. The –SH groups in the as-obtained porous PS frameworks were reacted with allyl-terminated PEG, thus leading to the formation of grafted PEG chains onto the pore walls with a 50% yield, as calculated by ^{1}H NMR (Figure 2d). Such a low yield was assumed to be likely due to the steric hindrance of the PEG$_{14}$-allyl macromolecule that did not allow for quantitative reaction yields. This functionalization assay illustrates the potential of such thiol-functionalized porous frameworks in the development of functional nanoreactors by thiol-ene "click" ligation with suitable ligands, *e.g.* imidazolyl moieties, allowing for further insertion of metallic nanoparticles within reactive supports for instance.

***In-situ* generation of gold nanoparticles adsorbed on porous polystyrene and supported catalytic reduction**

It is well-known that thiol-containing organic (macro)molecules have a strong affinity for gold surfaces.[42-45] In addition, supported gold nanoparticles (GNPs) are widely used as nanocatalysts for the reduction of nitro-containing compounds.[41] Notably, it has recently been reported by Barner-Kowollik's research group that thiol-coated nanoporous polystyrene obtained from PS-*b*-PEO diblock copolymers can tightly adsorb GNPs.[19] In this context, GNPs were *in-situ* generated on the surface of the as-obtained thiol-functionalized porous polystyrene frameworks. Nanoporous polymers were immersed for 3 days in a 1 wt. % chloroauric acid (HAuCl$_4$) solution, and then immediately subjected to hydride-mediated reduction in the presence of a solution of sodium borohydride in water. The presence of GNPs was verified by SEM (data not shown), and a quantification of gold in the hybrid system was realized by ICP-MS. It was observed that nanoporous polystyrene could adsorb ~ 1.5 wt. % of gold nanoparticles.

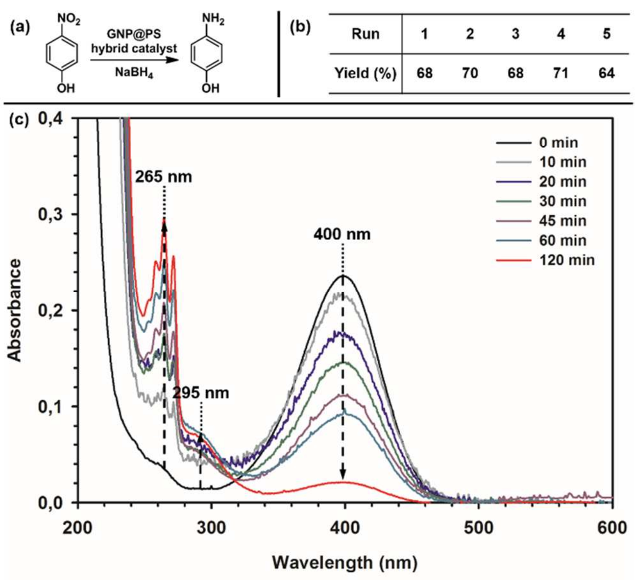

Run	1	2	3	4	5
Yield (%)	68	70	68	71	64

Figure 5. (a) Schematic reaction of the hydride-mediated GNP-catalyzed reduction of 4-nitrophenol. (b) Stability of the hybrid catalyst after 5 runs of the same reduction reaction. (c) UV-Vis spectra associated with the reduction of 4-nitrophenol into the corresponding 4-aminophenol as a function of reaction time in the presence of GNP@nanoporous PS hybrid catalyst.

Further, the catalytic behaviour of such hybrid porous systems was investigated. To this purpose, NaBH$_4$ and 4-nitrophenol were solubilized in water in the presence of the nanoporous GNP-adsorbed polystyrene hybrid catalyst (Figure 5a). The first run of 4-nitrophenol reduction into 4-aminophenol was achieved with a 68% yield over a 2 h period, as demonstrated by the dramatic decrease in the characteristic $\pi\rightarrow\pi^*$ transition band of 4-nitrophenol at 400 nm (Figure 5c). This clearly demonstrated the efficiency of the as-obtained catalyst. The UV-Vis spectrum corresponding to the blank experiment showed no reduction of the nitroaromatic compound, even after prolonged contact time with the thiol functionalized nanoporous frameworks (data not shown). Additionally, 4 successive reduction cycles were repeated following the same procedure. The catalyst efficiency was maintained, even after 5 runs (Figure 5b). These features clearly demonstrated that the nanoporous hybrid catalyst was very efficient and highly reusable.

Conclusions

Thiol-functionalized nanoporous materials could be engineered from novel PS-*b*-PLA diblock copolymers containing a disulfide bridge at the interface between the two distinct blocks. These copolymers were synthesized from a new asymmetric difunctional initiator, *i.e.* 2-[(2-hydroxyethyl)dithio]ethyl 2-bromoisobutyrate. After macroscopic orientation of the precursor copolymers and quantitative reduction of the disulfide bridge in a suitable solvent, well-defined nanoporous materials were obtained. The presence of thiol functions on the pore surface was demonstrated by EDX, and it allowed for further "click" thiol-ene-mediated functionalization of the resulting porous materials with an olefin-bearing model compound, *i.e.* allyl-terminated PEG. More interestingly, thiol-coated nanoporous polymeric frameworks allowed for the robust immobilization of gold nanoparticles at the surface of the nanochannels, and such hybrid systems could efficiently be used as supported catalysts for the reduction of nitro compounds.

This investigation paves the way for further functionalization of thiol-coated porous nanoreactors with interesting model compounds that could find applications in the design of innovative catalytic supports or nanofiltration membranes.

Notes and references

Institut de Chimie et des Matériaux Paris-Est, CNRS-Université Paris-Est Créteil, 2 rue Henri Dunant, 94320 Thiais, France.
E-mail: ledroumaguet@icmpe.cnrs.fr; Fax: +33 (0)1 49 78 12 08; Tel: +33 (0)1 49 78 11 77

1. D. Wu, F. Xu, B. Sun, R. Fu, H. He and K. Matyjaszewski, *Chem. Rev.*, 2012, **112**, 3959-4015.
2. J. Guan, K. L. Fujimoto, M. S. Sacks and W. R. Wagner, *Biomaterials*, 2005, **26**, 3961-3971.
3. H. P. Hentze and M. Antonietti, *Rev. Mol. Biotechnol.*, 2002, **90**, 27-53.
4. C. R. Martin, *Science*, 1994, **266**, 1961-1966.
5. M. A. Hillmyer, *Adv. Polym. Sci.*, 2005, **190**, 137-181.
6. D. A. Olson, L. Chen and M. A. Hillmyer, *Chem. Mater.*, 2008, **20**, 869-890.
7. T. Pietsch, N. Gindy, B. Mahltig and A. Fahmi, *J. Polym. Sci., Part B: Polym. Phys.*, 2010, **48**, 1642-1650.
8. K. A. Cavicchi, A. S. Zalusky, M. A. Hillmyer and T. P. Lodge, *Macromol. Rapid Commun.*, 2004, **25**, 704-709.
9. M. Hansen, M. Vigild, R. Berg and S. Ndoni, *Polym. Bull.*, 2004, **51**, 403-409.
10. P. P. Szewczykowski, K. Andersen, L. Schulte, K. Mortensen, M. E. Vigild and S. Ndoni, *Macromolecules*, 2009, **42**, 5636-5641.
11. J. L. Hedrick, R. D. Miller, C. J. Hawker, K. R. Carter, W. Volksen, D. Y. Yoon and M. Trollsås, *Adv. Mater.*, 1998, **10**, 1049-1053.
12. S.-Y. Chen, Y. Huang and R. C.-C. Tsiang, *J. Polym. Sci., Part A: Polym. Chem.*, 2008, **46**, 1964-1973.
13. R. Sekine, N. Sato, T. Matsuyama, S. Akasaka and H. Hasegawa, *J. Polym. Sci., Part A: Polym. Chem.*, 2007, **45**, 5916-5922.
14. Y. Li and T. Ito, *Langmuir*, 2008, **24**, 8959-8963.
15. A. S. Zalusky, R. Olayo-Valles, C. J. Taylor and M. A. Hillmyer, *J. Am. Chem. Soc.*, 2001, **123**, 1519-1520.
16. A. S. Zalusky, R. Olayo-Valles, J. H. Wolf and M. A. Hillmyer, *J. Am. Chem. Soc.*, 2002, **124**, 12761-12773.
17. D. Grande, J. Penelle, P. Davidson, I. Beurroies and R. Denoyel, *Microporous Mesoporous Mater.*, 2011, **140**, 34-39.
18. R. Majdoub, T. Antoun, B. Le Droumaguet, M. Benzina and D. Grande, *React. Funct. Polym.*, 2012, **72**, 495-502.
19. M. Glassner, J. P. Blinco and C. Barner-Kowollik, *Polym. Chem.*, 2011, **2**, 83-87.
20. M. Kang and B. Moon, *Macromolecules*, 2008, **42**, 455-458.
21. H. Zhao, W. Gu, M. W. Thielke, E. Sterner, T. Tsai, T. P. Russell, E. B. Coughlin and P. Theato, *Macromolecules*, 2013, **46**, 5195-5201.
22. M. Zhang, L. Yang, S. Yurt, M. J. Misner, J. T. Chen, E. B. Coughlin, D. Venkataraman and T. P. Russell, *Adv. Mater.*, 2007, **19**, 1571-1576.
23. C. A. Fustin, B. G. G. Lohmeijer, A. S. Duwez, A. M. Jonas, U. S. Schubert and J. F. Gohy, *Adv. Mater.*, 2005, **17**, 1162-1165.
24. A. Takahashi, Y. Rho, T. Higashihara, B. Ahn, M. Ree and M. Ueda, *Macromolecules*, 2010, **43**, 4843-4852.
25. J.-H. Ryu, S. Park, B. Kim, A. Klaikherd, T. P. Russell and S. Thayumanavan, *J. Am. Chem. Soc.*, 2009, **131**, 9870-9871.
26. R. N. Keller and H. D. Wycoff, Inorganic Synthesis, John Wiley, New York, 1946, pp 1–4.
27. J. Ramier, E. Renard and D. Grande, *Macromol. Chem. Phys.*, 2012, **213**, 784-788.
28. J. Ramier, E. Renard and D. Grande, *J. Polym. Sci., Part A: Polym. Chem.*, 2012, **50**, 1445-1455.
29. P. Kurian, S. Zschoche and J. P. Kennedy, *J. Polym. Sci., Part A: Polym. Chem.*, 2000, **38**, 3200-3209.
30. J.-S. Wang and K. Matyjaszewski, *J. Am. Chem. Soc.*, 1995, **117**, 5614-5615.
31. M. Kato, M. Kamigaito, M. Sawamoto and T. Higashimura, *Macromolecules*, 1995, **28**, 1721-1723.
32. H. R. Kricheldorf, I. Kreiser-Saunders and C. Boettcher, *Polymer*, 1995, **36**, 1253-1259.
33. N. V. Tsarevsky and K. Matyjaszewski, *Macromolecules*, 2002, **35**, 9009-9014.
34. N. V. Tsarevsky and K. Matyjaszewski, *Macromolecules*, 2005, **38**, 3087-3092.
35. P. L. Drzal, J. D. Barnes and P. Kofinas, *Polymer*, 2001, **42**, 5633-5642.
36. N. V. Tsarevsky, J. Huang and K. Matyjaszewski, *J. Polym. Sci., Part A: Polym. Chem.*, 2009, **47**, 6839-6851.
37. H. Gao, N. V. Tsarevsky and K. Matyjaszewski, *Macromolecules*, 2005, **38**, 5995-6004.
38. J. A. Burns, J. C. Butler, J. Moran and G. M. Whitesides, *J. Org. Chem.*, 1991, **56**, 2648-2650.
39. Y. Chujo, K. Sada, A. Naka, R. Nomura and T. Saegusa, *Macromolecules*, 1993, **26**, 883-887.
40. W. Wang and R. W. Murray, *Langmuir*, 2005, **21**, 7015-7022.
41. A. B. Lowe, *Polym. Chem.*, 2010, **1**, 17-36.
42. N. Pradhan, A. Pal, T. Pal, *Langmuir,* 2001, 17, 1800-1802.
43. S. Panigrahi, S. Basu, S. Praharaj, S. Pande, S. Jana, A. Pal, S.K. Ghosh, T. Pal, *J. Phys. Chem. C*, 2007, **111**, 4596-4605.
44. K. Kuroda, T. Ishida, M. Haruta, *J. Mol. Catal. A - Chem.*, 2009, **298**, 7-11.
45. S. Saha, A. Pal, S. Kundu, S. Basu, T. Pal, *Langmuir*, 2009, **26**, 2885-2893.

Thiol-coated nanoporous materials were successfully engineered from diblock polystyrene-*block*-poly(D,L-lactide) precursors possessing a disulfide junction. The further immobilization of GNPs at the pore surface provided novel supported nanocatalysts for the efficient reduction of *p*-nitrophenol.